Mater.Phys.Mech. 6 (2003) 49-57

SEMIGRAND CANONICAL MONTE CARLO SIMULATION WITH GIBBS-DUHEM INTEGRATION TECHNIQUE FOR ALLOY PHASE DIAGRAMS

Atsushi Mori[1], Brian B. Laird[2], Yoshihiro Kangawa[3], Tomonori Ito[4] and Akinori Koukitu[3]

[1]Department of Optical Science and Technology, Faculty of Engineering, The University of Tokushima, Tokushima 770-8506, Japan
[2]Department of Chemistry, University of Kansas, Lawrence, KS 66045, U.S.A.
[3]Department of Applied Chemistry, Faculty of Engineering, Tokyo University of Agriculture and Technology, Tokyo 184-8588, Japan
[4]Department of Physics Engineering, Faculty of Engineering, Mie University, Mie 514-8507, Japan

Received: December 03, 2002

Abstract. Formulation is given for the Gibbs-Duhem integration (GDI) method in the semigrand canonical (SGC) ensemble, in which the total number of particles N is fixed with the specified chemical potential differences between species $\Delta\mu_i$ ($\equiv\mu_i-\Delta\mu_1$;i=2,3,...). Demonstration of the SGC Monte Carlo simulation with the GDI technique is given for a pseudo-binary semiconductor alloy, $In_xGa_{1-x}N$.

1. INTRODUCTION

Phase diagrams are inevitable materials in materials processing. We look into the phase diagrams when we determine the condition of chemical syntheses, crystal growth, device fabrication, and so on. Nothing can be started without knowing the melting temperature in the crystal growth from the melt. Without appropriate phase diagrams one cannot process materials successfully. To control the composition of material so that expected properties are realized, the phase boundary in the alloy phase diagram must be sufficiently accurate. In recent development of nano-technologies requirement to accurate phase diagrams is increasing. For some novel materials there exist no accurate phase diagrams or its accuracy is insufficient. In such case one may expect computational methods to make an appropriate phase diagram. InGaN, to which we have applied the method presented in this paper, is a typical example; there exist several phase diagrams obtained on the basis of an approximate theory such as the regular solution model. The purpose of this paper is, however, to present a computational method to search the phase boundary.

Computer simulations such as molecular dynamics and Monte Carlo (MC) simulations to investigate the phase behavior have greatly been developed recently. So far, thermodynamic integration (TI) method was used to calculate the phase equilibrium condition. In TI a free energy is calculated by integration along a path connecting a reference state to states of interest. Hoover and Ree [1] early proposed the single-occupancy cell method; a system composed of cells in each of which a particle lies was employed as a reference. This method was successfully applied to locate the hard-sphere crystal-melt phase transition point [2] and the melting line of the Lennard-Jones system [3]. Frenkel and Ladd [4] proposed the harmonic crystal as a reference and applied it to the hard-sphere system.

TI requires numbers of samplings by simulations along a path connecting the reference state to the states of interest. Therefore, computational task is so heavy and accordingly the accuracy is not so high. In this respect, the direct phase equilibrium

Corresponding author: Atsushi Mori, e-mail: mori@opt.tokushima-u.ac.jp

simulation without two-phase interface, the Gibbs ensemble MC (GEMC) method, devised by Panagiotopoulos [5] in 1987 was a progress; computational tasks was reduced and at a same time accuracy was increased. GEMC simulations are, thus, extensively used even now. Beside its success GEMC method has a shortcoming. One simultaneously performs MC runs, number of which equals that of coexisting phases, with interaction among coexisting phases. One of such interaction is particle exchange among them. Therefore, one encounters, as in the grand canonical MC simulation, difficulty in insertion of a particle when the system is dense [6].

Kofke and Glandt [7] stimulated a development of the semigrand canonical MC (SGCMC) simulation. As mentioned in a review [8] SGC formalism, however, appeared early in 1970 in a quite generalized thermodynamic argument for multicomponent systems by Griffiths and Wheeler [9]. Later but earlier than Kofke and Glandt [7] SGC formalism was given for polydisperse fluids by Bariano and Glandt [10]. There was a development of SGCMC simulation along this line [11-13].

In view of simulation of the phase coexistence SGCMC method is an indirect one. Nevertheless, it is recently applied to the phase coexistence involving solid phase because, unlike GEMC and the grand canonical MC simulations, particle insertion MC moves are not necessary. Instead, species-identity changes are attempted, which for a binary case is equivalent to the spin flip procedure in the kinetic Ising model of Grauber's dynamics. The identity change MC moves are attempted under a given chemical potential difference, $\Delta\mu$, which corresponds to the magnetic field in the Ising model. In the Ising system below the Curie temperature the two-phase equilibrium – equilibrium between phases of up-spin rich and down-spin rich – condition coincides to the zero magnetic field condition. This is due to the symmetry with respect to up-spin–down-spin conversion. Zero chemical potential difference, $\Delta\mu=0$, gives two phase equilibrium only in the molecular systems with the intermolecular potentials possessing a corresponding symmetry [$\phi_{AA}=\phi_{BB}\neq\phi_{AB}$ with ϕ_{ij} ($i,j=A,B$) being the intermolecular potentials between species i and j] as pointed out already [14-17]. SGCMC simulation is, thus, convenient for such cases. Indeed, liquid–liquid [14-20] phase equilibria in symmetrical mixtures were investigated by SGCMC simulation with this help. If there is not symmetry determining the equilibrium condition prior to the simulation, one needs a procedure which determines the equilibrium condition such as TI as performed early for vapor–liquid phase equilibria [7,21,22]. (Because fugacity fraction was used instead of the chemical potential difference, despite the symmetry the SGC free energies were computed as functions of the fugacity fraction.) The SGC free energies, Y's, are to be calculated as a function of $\Delta\mu$ at fixed T and P and then equalities of Y's among coexisting phases are to be solved for $\Delta\mu$.

Only if the coexistence region is so narrow as its width is smaller than numerical errors, the coexistence region itself can be regarded as the equilibrium point with the error. De Miguel *et al.* [23] investigated ternary liquid mixture. Due to the symmetric intermolecular interaction one of two chemical potential differences vanished. Though the other was not vanished, TI was not performed. Discontinuity in the equation of state was also used by Bate and Frenkel [24] in a polydisperse system.

As mentioned in [7], unless the ensemble is of isothermal–isobaric SGC (if so, due to the Gibbs phase rule, number of coexisting phases turns to be 1), GEMC simulation is possible in SGC ensemble. This is an alternative way of finding out the phase equilibrium condition. GEMC in SGC ensemble was already performed early by Stapleton *et al.* [25] and recently by Bate and Frenkel [26].

There was another route along which SGCMC was developed: as opposed to in previous paragraphs, SGC may be organized as incorporation of atomic moves into the Ising-type lattice gas model. Foils [27] performed SGCMC simulation for Ni-Cu binary alloy in 1985. He investigated how surface segregation was enhanced relative to the segregation in the bulk; alloy phase diagram was not calculated. Later in 1989 Kelieres and Tersoff [28] performed SGCMC simulation for the Si-Ge binary system; an alloy phase diagram was obtained by detecting a sufficiently small miscbility gap region as done in [23,24]. Recently reinvestigation with this simplified rough estimate for the same system with large system size was carried out by Laradji *et al.* [29]. Notable work on the alloy phase diagram was that of Dünweg and Landau [30], who attained TIs (those described in Secs. 2.1 and 2.2).

The other method, which also enables the simulations of dense systems, developed in the last decade was the Gibbs-Duhem integration (GDI) technique formulated by Kofke [31,32] (see also [8]). GDI for the *T-P* phase diagram of one-component systems is nothing other than a numerical integration of Clausius-Clapeyron's equation along a two-phase equilibrium condition. (Therefore, GDI may be referred to as Clausius-Clapeyron integration

[33,34].) GDI technique has versatility; it was applied to not only the systems with difficulty in simulation such as dense phases. Sturgeon and Laird [35] accomplished adjustment of potential parameters by GDI technique, which inspired the present work – GDI in SGC ensemble for the alloy phase diagram. Potential parameter adjustment may be regarded as an extension of previous studies [36-39], in which the phase transition lines were traced in the space including a potential-parameter axis.

Formalism of GDI was first extended to multicomponent systems by Mehta and Kofke [22]. They formulated also in an "osmotic" ensemble (number of solute particles were fixed instead of total number of molecules); MC simulations for vapor-liquid coexistence in binary Lennard-Jones systems were demonstrated in SGC as well as osmotic ensembles. Following Kofle [31,32], they proposed the infinite dilution as a starting point of GDI; Henry's law was to be used to predict an adjacent point. Recently Hitchcock and Hall [40] preformed GDI for solid-liquid coexistence of binary Lennard-Jones mixtures with estimation of Henry's constant by simulation. While Mehta and Kofke [22] described a Clapeyron-type equation at constant T, Escobedo and a co-worker [41-43] gave a general form and then rewrote it in an isobaric form. Escobedo and Pablo [41], however, performed GDI in $NV\mu_1\mu_2$ (grand canonical) ensemble for liquid-liquid coexistence for binary system of short chains with symmetric interactions. Escobedo [42,43] investigated vapor-liquid coexistence of binary and ternary mixtures by GDI also in a grand canonical ensemble.

The remainder of this paper is organized as follows. We define SGC ensemble in Sec. 2.1 and explain GDI technique in Sec. 2.2. Formalism of GDI in SGC ensemble is, at first, given for a c-component isobaric SGC ensemble in Sec. 2.3. In Sec. 2.4 the formulation is simplified for a binary case. Outline of the simulation of $In_{1-x}Ga_xN$ pseudo binary semiconductor alloy and its result are given in Sec. 3. Sec. 4 includes a summary and concluding remarks.

2. FORMULATION

2.1. Semigrand canonical ensemble

Let us consider a c-component system. In the grand canonical ensemble the chemical potentials of all components,$\{\mu_i;\ i=1,...,c\}$, are specified and numbers of particles of every components vary independently. On the other hand, in the canonical ensemble total numbers of particles of each component, $\{N_i;\ i=1,...,c\}$, are fixed. SGC ensembles are defined as a statistical ensemble lying between these. In the isobaric SGC ensemble $\Delta\mu_i$ ($\equiv\mu$-$\Delta\mu;i=2,...,c$),P, and T are specified with a conserved total number of particles $N(\equiv \sum_{i=1}^{c} N_i)$. Therefore, the composition or the molar fraction $\{x_i\}\equiv\{N_i/N;i=2,...,c\}$ varies through $\{N_i\}$ varying under a constraint of $\sum_{i=1}^{c} N_i = N$ fixed.

The isobaric SGC partition function is defined as

$$Q_{N\{\Delta\mu\}PT} = \sum_{N_2}\cdots \sum_{N_c}\int dV \exp\left[\beta\left(\sum_{i=2}^{c} N_i\Delta\mu_i - PV\right)\right] Q_{(N-\sum_{i=2}^{c} N_i)N_2\ldots N_cVT}, \quad (1)$$

where $\beta\equiv 1/k_BT$ and $Q_{N_1N_2\ldots N_cVT}\equiv Z_{N_1\ldots N_c}/\prod_{i=1}^{c} N_i!\,\Lambda_i^{3N_i}$ is the canonical partition function with the configurational integral

$$Z_{N_1\ldots N_c} \equiv \int d^{N_1}r\cdots d^{N_c}r \exp[-\beta U_{N_1-N_c}], \quad (2)$$

and the thermal de Broglie wavelength $\Lambda_i \equiv h/\sqrt{2\pi m_i k_B T}$. $U_{N_1\ldots N_c}$ in Eq. (2) represents the potential energy of system containing N_i particles of species i(i=1,...c).

SGC free energy [7] is defined by

$$Y(N,\{\Delta\mu\},P,T) = -k_BT\ln Q_{N\{\Delta\mu\}PT}. \quad (3)$$

The following thermodynamic relation [9] is readily derived by differentiating Eq. (3) with the help of Eq. (1):

$$\frac{\partial Y}{\partial(\Delta\mu_i)} = \langle N_i\rangle = Nx_i; \quad i = 2,\ldots,c, \quad (4)$$

where $\langle\bullet\bullet\rangle$ denotes the isobaric SGC average:

$$\langle\bullet\bullet\rangle \equiv \frac{1}{Q_{N\{\Delta\mu\}PT}}\sum_{N_2}\cdots\sum_{N_c}\int dV(\bullet\bullet) \exp\left[\beta\left(\sum_{i=2}^{c} N_i\Delta\mu_i - PV\right)\right] Q_{(N-\sum_{i=2}^{c} N_i)N_2\ldots N_cVT}. \quad (5)$$

Let us perform the Legendre transformation [7,10] here. At first, we regard the Gibbs free energy G as a function of $N_2,...,N_c,P$ and T. Thus, we have

$$\frac{\partial}{\partial N_j} G\left(N - \sum_{i=2}^{c} N_i, N_2,\ldots,N_c,P,T\right) = \mu_j - \mu_1 = \Delta\mu_j; \quad j = 2,\ldots,c. \quad (6)$$

Then,

$$Y = G - \sum_{i=2}^{c} N_i \Delta\mu_i = \sum_{i=1}^{c} N_i \mu_i - \sum_{i=2}^{c} N_i (\mu_i - \mu_1) = N\mu_1. \quad (7)$$

Accordingly, SGC free energy Y is turned to be nothing other than the chemical potential of species 1 itself [9].

We write the Gibbs-Duhem relation, which plays a key role in GDI, into the form:

$$d\mu_1 = -sdT + vdP - \sum_{i=2}^{c} x_i d(\Delta\mu_i), \quad (8)$$

where $s \equiv S/N$ and $v \equiv V/N$.

We can detect the phase equilibrium "point" $\Delta\mu^{eq}(T,P)$ by the equality of SGC free energies or μ_1's among the coexisting phases. TI based on thermodynamic relation is to be utilized; Eq. (4) is integrated by x_i at a fixed T and P to give a free energy difference.

2.2. Gibbs-Duhem integration for one-component two-phase coexistence

Recalling the Gibbs-Duhem relation for single component system [Eq. (8) without the last term] we write Clapeyron's equation:

$$\frac{dP^{eq}}{dT} = \frac{\Delta s}{\Delta v} = \frac{\Delta h}{T\Delta v}, \quad (9)$$

where Δ denotes the difference between two coexisting phases I and II. The superscript "eq" here and hereafter indicates the equilibrium between those coexisting phases; P^{eq} is the equilibrium pressure of phases I and II at temperature T. To get the last expression we have used $\Delta\mu \equiv \Delta h - T\Delta s = 0$ at equilibrium with h denoting the molecular enthalpy, i.e., the latent heat of the phase transition per molecule. Once one knew a point on the phase coexisting line, say (T,P), one can predict an adjacent point on the coexistence line, $(T+dT, P+dP)$, with the help of Eq. (9).

The last expression on Eq. (9) can be evaluated by two separate simulations for coexisting two phases. One needs no particle insertion procedure. Predictor-corrector scheme is often used in integrating Eq. (9), i.e., the adjacent point(s) may be re-evaluated by using the Δh and Δv values at the predicted point(s). Several formulations were already given by Kofke [31,32].

2.3. Gibbs-Duhem integration in *c*-component semigrand canonical ensemble

Remember the Gibbs-Duhem relation for the c-component system, Eq. (8), and follow the derivation of Clausius-Clapeyron's equation. Let us consider ϕ phase (phases I,II,...,ϕ) coexistence at $(T,P,\{\Delta\mu\})$ and $(T+dT,P+dP,\{\Delta\mu+d(\Delta\mu)\})$. Subtracting $\mu_1^j(T,P,\{\Delta\mu\}) = \mu_1^{\mathrm{I}}(T,P,\{\Delta\mu\})$ from $\mu_1^j(T+dT,P+dP,\{\Delta\mu+d(\Delta\mu)\}) = \mu_1^{\mathrm{I}}(T,P,\{\Delta\mu+d(\Delta\mu)\})$ for j=II,...,ϕ we obtain the following set of equations up to first order, where superscripts on μ_1 and those on x_i, h, and v in Eq. (10) represent the phase.

$$\sum_{i=2}^{c} \Delta x_i^j d(\Delta\mu_i^{eq}) = -\frac{\Delta h^j}{T} dT + \Delta v^j dP; \quad j = \mathrm{II},\ldots,\phi. \quad (10)$$

where $\Delta x_i^j \equiv x_i^j - x_i^{\mathrm{I}}$, $\Delta h^j \equiv h^j - h^{\mathrm{I}}$, and $\Delta v^j \equiv v^j - v^{\mathrm{I}}$. We have replaced Δs^j by $\Delta h^j/T$ as done in obtaining the last expression on Eq. (9).

Eq. (10) should be treated as simultaneous equations. For isobaric (dP=0) case, for example, we can solve them for $d(\Delta\mu_i^{eq})$ by calculating the inverse matrix of (Δx_i^j). Of course, if the number of coexisting phases, ϕ, is less than the number of component c, then these simultaneous equations are underdetermined, and in the opposite case overdetermined. All matrix elements Δx_i^j as well as Δh^j and Δv^j can be evaluated by separate ϕ simulations for coexisting phases. Thus, one can predict an adjacent "point" on a phase coexistence "line." Only in the cases of isobaric SGC simulations one benefits from this formulation. Or, in an isochoric SGC case one has to determine the volumes of every coexisting phase so that the mechanical equilibrium, i.e., equality of pressures among phases, is satisfied at every step of GDI.

2.4. Gibbs-Duhem integration for two-component two-phase coexistence

Let us simplify the formulation by limiting ourselves to a binary system, and put ourselves toward an application. We consider coexistence between phases I and II in a system of components 1 and 2. The Gibbs-Duhem relation reduces to

$$d\mu_1 = -sdT + vdP - xd(\Delta\mu), \quad (11)$$

where we omitted the subscript "2" under x and $\Delta\mu$. Also, Eq. (10) reduces to

$$\Delta x d\left(\Delta\mu_i^{eq}\right) = -\frac{\Delta h}{T}dT + \Delta v dP, \qquad (12)$$

where $\Delta x \equiv x^{II}-x^{I}$, $\Delta h \equiv h^{II}-h^{I}$, and $\Delta v \equiv v^{II}-v^{I}$. Thus, in the isobaric case, we have the equation to be integrated in T-$\Delta\mu$ plane:

$$\frac{d(\Delta\mu^{eq})}{dT} = -\frac{\Delta h}{T\Delta x}. \qquad (13)$$

The equation to be integrated in P-$\Delta\mu$ plane, which gives alternatively a x-P phase diagram at a fixed T, is also readily obtained. Mahta and Kofke [22] described this equation in terms of the fugacity fraction in place of $\Delta\mu$. The reason why the Clapeyron-type equation is written in terms of P may be for convenience in applying the Henry's law.

3. DEMONSTRATION

SGCMC simulation with GDI technique has been demonstrated for a pseudo-binary semiconductor alloy, InGaN. We have investigated InGaN pseudomorphic to the basal plane of a wulzite GaN substrate. In InGaN pseudo-binary case, I and II represent the Ga-rich and In-rich phases, respectively. In addition, we note that GaN and InN are treated as the components 1 and 2, respectively. In Sec. 3.1 the empirical interatomic potential is given and system investigated is described. The result of TI at 800K, which has been used as an initial condition of GDI, is presented in Sec. 3.2. Result of GDI and discussion are given in Sec. 3.3.

3.1. Simulation model and system

The empirical interatomic potential [44] used in this simulation has the form [45]

$$V_{ij} = A\exp[-\beta(r_{ij}-R_i)^{\gamma}][\exp(-\theta r_{ij}) - B_0\exp(-\lambda r_{ij})G(\eta)/Z_i^{\alpha}], \qquad (14)$$

where r_{ij} is the interatomic distance between atoms i and j, R_i is the minimum distance between atoms, $Z_i=\Sigma_j \exp[-\beta(r_{ij}-R_i)^{\gamma}]$ is the effective coordination number of atom i, and $G(\eta)$ is the bond bending term for tetrahedrally bonded atom pairs. (Do not confuse β in Eq.(14) with the reciprocal temperature.) For the values of potential parameters, see also [46].

Excess energy, $\Delta E(x)=E(x)-[xE_{InN}+(1-x)E_{GaN}]$, was already calculated [46]. x-ΔE curve is of vary asymmetric shape; the maximum point is significantly shifted to In-rich side. In this calculation as well as in the present simulation atomic positions parallel to the substrate were fixed. Only normal positions were allowed to move. Corresponding to the decrease of the degree of freedom due to this constraint, the exponent $3N_i$ on the thermal de Broglie wavelength in the denominator of the canonical partition function $Q_{\{Ni\}VT}$ is changed into N_i. In the present simulation the vertical system size, L_z, was moved using random numbers with the pseudo-Boltzmann weight at P=1 atm. Maximum displacements of z-position moves and L_z-move in the present SGCMC simulation were determined so that the acceptance ratios lay in 0.35~0.50. Lateral sizes of the basal plain (xy-direction) were L_x=25.67Å and L_y=22.14Å. Periodic boundary condition was imposed in all three directions. The total number of atoms was N_{tot}=1024. We confirmed that $\Delta E(x)$ converges with N within a numerical error around N_{tot}=512 [46]. Saturation of the system size effect on the energy does not necessarily mean that on the free energy. As a possibility, entropy may have much large system size dependence. However, to reduce the computation time we relied on our previous result [46].

3.2. Thermodynamic integration

Fig. 1 is the $\Delta\mu$-x relation at T=800K. All simulations were started from pure GaN or InN and then continued for 2~6·10^6 MC cycles (MCCs). Here, one MCC contains one position move per atom on average and one volume move. Each point in the gap region for the Ga-rcih branch in Fig. 1 was obtained by averaging over 5~10 independent simulations. Evolution of the composition, the system size, and the system energy with MCC were monitored. Multi-step relaxation was sometimes observed for the Ga-rich branch, which indicated a multi-valley free energy structure. Suprelattice stacking along c-axis was observed, e.g., IGGGGIGG with I and G denoting respectively In-rich and Ga-rich layers parallel to the basal plane. (The system includes 8 layers in z-direction.) Concerning such superlattice structure in a finite system, we cannot distinguish some superlattice structures of a periodicity longer then the system size with some suprelatice structures including stacking faults. Some samples with two or more successive In-rich layers laying in a Ga-rich system were excluded in the sampling average, because those were not distinguished with the phase separation. Samples including a In-rich layer were included in the averaging, though the superlattice periodicity may exceed the system

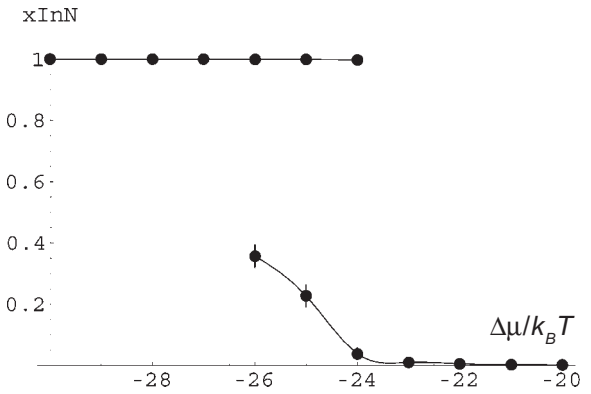

Fig. 1. Indium composition x is plotted against $\Delta\mu/k_BT$ at 800K. Bistability is observed in a region $\Delta\mu/k_BT$=-26~-24. Lines are the Spline curves.

size. At apparent it seems that average was taken over distinct (mata)stable states. It may be, however, regarded that we sampled parts with no, one, or several In-rich layers from a long-preriodicity superlattice structure. In this sense Fig. 1 is not the final result. We note that an In-rich layer includes several Ga atoms. It means that, for example, the In composition of IGGGIGGG... is not necessarily 0.25. We will not compare the superlattice structure with the experimentally observed order [47-49].

Nevertheless, the result seems reasonable. Bistabiltiy is clearly seen in Fig. 1. To determine the equilibrium $\Delta\mu$ we performed TIs. In addition to $\Delta\mu$-integration (of Eq. (4))

$$\mu_1(\Delta\mu) - \mu_1(\Delta\mu_0) = \int_{\Delta\mu_0}^{\Delta\mu} x d(\Delta\mu), \tag{15}$$

along the lines in Fig. 1, we calculated the SGC free energies at $\Delta\mu$=-30k_BT($\equiv\Delta\mu_0^{II}$) for In-rich branch and $\Delta\mu$=-20k_BT ($\equiv\Delta\mu_0^{I}$) for Ga-rich one using the harmonic crystals [4] as references as follows. We note here, before describing this, that $\Delta\mu_1$=Y/N with N=N_{In}+N_{Ga} being the total number of cation-anion pairs.

Let U_0 be the harmonic potential. We replace $U_{N_{GaN}N_{InN}}$ in the equation corresponding to Eq. (2) by

$$U(\lambda) = \lambda U_{N_{GaN}N_{InN}} + (1-\lambda)U_0 . \tag{16}$$

We have readily

$$\frac{\partial Y}{\partial \lambda} = \langle U_{N_{GaN}N_{InN}} + U_0 \rangle_\lambda , \tag{17}$$

where $\langle \bullet\bullet \rangle_\lambda$ denotes SGC average with $U(\lambda)$ used as the interatomic potential. Accordingly, we calculated SGC free energies respectively at $\Delta\mu_0^{II}$ for In-rich branch and $\Delta\mu_0^{I}$ for Ga-rich branch by the following equation:

$$Y(\Delta\mu_0;1) - Y(\Delta\mu_0;0) = \int_0^1 \langle U_{N_{GaN}N_{InN}} - U_0 \rangle_\lambda d\lambda . \tag{18}$$

where $Y(\Delta\mu_0;\lambda)$ is Y of the system with the interaction $U(\lambda)$. Also due to the fact that U_0 is the harmonic crystal, $Y(\Delta\mu_0^{II};0)$-$Y(\Delta\mu_0^{I};0)$ can be calculated as a function of $\Delta\mu_0^{I}$ and $\Delta\mu_0^{II}$:

$$Y(\Delta\mu_0^{II};0) - Y(\Delta\mu_0^{I};0) = Nk_BT \ln \frac{1+\sqrt{m_{In}/m_{Ga}}\exp(\beta\Delta\mu_0^{II})}{1+\sqrt{m_{In}/m_{Ga}}\exp(\beta\Delta\mu_0^{I})}, \tag{19}$$

where m_{In} and m_{Ga} are the masses of In and Ga, respectively. Suppression of the lateral degree of freedom has affected Eq. (19). In three dimensionally movable cases masses should be cubed. It should be noted that in Eq. (19) the masses in the square root symbols are not those of cation-anion pairs.

$\langle U_{N_{GaN}N_{InN}} - U_0 \rangle_\lambda / N_{tot}$ was plotted against λ for Ga-rich and In-rich branches respectively at $\Delta\mu/k_BT$= -20 and -30 (their figures are not presented in this paper). Ten-point Gauss-Legendre quadrature was employed for λ-integration. Performing $\Delta\mu$- and λ-integrations we determined $\Delta\mu^{eq}/k_BT$= -25.19 at T=800K. For $\Delta\mu$-integration the $\Delta\mu$-x curve was fitted by a Spline curve. Difference between the result of the Spline fit and that of connecting linear interpolating lines was 0.019 in $\Delta\mu^{eq}/k_BT$. We should note here that Dünweg and Landau [30] made a use of values of composition fluctuation ($\langle x^2 \rangle - \langle x \rangle^2 \equiv \delta(x^2)$) to fit the $\Delta\mu$-x curves via the relation between $\Delta\mu$-derivative of x and $\delta(x^2)$. (Equilibrium composition fluctuation is found to be proportional to the slope of the $\Delta\mu$-x curve. Derivation is an easy exercise; one may only differentiate Eq. (4) again.) In the present simulation, however, the composition fluctuation was not accurately evaluated.

3.3. Result of Gibbs-Duhem integration

We performed GDI using the result of the preceding subsection as a starting point. Predictor-corrector scheme corresponding to the trapezoid formula was employed. We simulated several points (for several $\Delta\mu$ at a temperature) around predicted one and then made linear interpolation to the predicted point and, in turn, to the corrected point. The linear interpola-

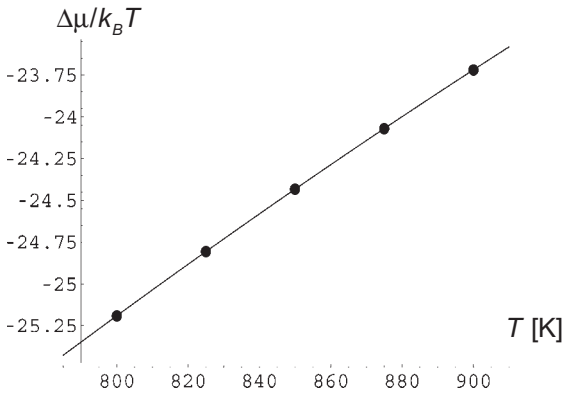

Fig. 2. $\Delta\mu^{eq}$-T relation as a result of the Gibbs-Duhem integration. The result from the thermodynamic integration, $\Delta\mu/k_BT$=-25.19 at T=800K, was used as the starting point. An almost linear relation is seen.

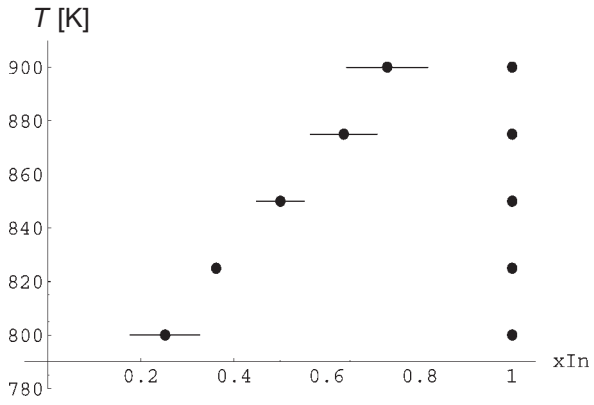

Fig. 3. x-T "phase diagram" obtained by sampling along the coexistence line in Fig. 2. Only terminal compositions at simulated temperatures are plotted. We see, however, clearly a shift of the two-phase region toward the In-rich side.

tion was unfortunately not succeeded for Ga-rich branch at T=850, 875, and 900K. (There were no significant $\Delta\mu$-dependence of the composition for In-rich branch.) Instead of linear interpolation average was taken over all simulation results at a temperature for Ga-rich branch. This is indicated by error bars in x-T phase diagram (Fig. 3). Thus, the predictor-corrector did not affect the composition except for T=825K but T-$\Delta\mu^{eq}$ relation (Fig. 2). If we have numbers of samplings enough to make a histogram of distribution of state variables at each $\Delta\mu$, we can utilize the histogram reweighting method [50] as suggested by Escobedo [43] (also in SGCMC simulation as Gelv et al. [18] done). Unfortunately, we had not enough number of samplings. Length of a simulation was $2\sim6\cdot10^6$ MCCs and we repeated simulations 3~7 times for a point. Similarly to the 800K samples superlattice structures were observed. Averaging procedure was the same. T-$\Delta\mu^{eq}$ relation and x-T phase diagram are shown in Figs. 2 and 3, respectively. $\Delta\mu^{eq}/k_BT$ increases almost linearly with T. On the other hand, x-T phase diagram is highly asymmetric, which reflects the asymmetric nature of the excess energy curve [46]. The In-rich side portion of the excess energy curve forms deep and narrow valley. Less-sensitivity of composition of In-rich phase on the temperature is interpreted as the less entropy gain due to Ga incorporation into In-rich phase which cannot overcome the energy gain of climbing a steep energy slope. Shape of the Ga-rich phase boundary is not that expected from the regular solution model: the slope of the boundary does not decreasd with T monotonicaly. A similar behavior for the InGaN binordal curve has been obtained by Teles et al. [52] using a cluster expansion method with a quantum mechanical calculation. Not only the energy but also the number of (meta)stable states allowed for a supercell of the quantum mechanical calculation were evaluated.

4. CONCLUDING REMARKS

We summarize the present work as follows:

- Formulation of the Gibbs-Duhem integration in the c-component semigrand canonical ensemble has been given.
- As a demonstration alloy phase diagram of $In_xGa_{1-x}N$/GaN has been investigated.

We discuss a remainder problem. As pointed in Sec. 3.2 we encountered the multi-valley free energy phenomena. Why we started all simulation with pure GaN or InN was to avoid the initial condition sensitivity. Or, if we started a simulation with a configuration obtained by a previous run, the system must be trapped by a metastable valley near that of the previous run. The multi-valley structure may be interpreted by regarding the system as a huge chemical bond network. There are a lot of ways of deformation when the other atoms are mixed. This resembles chain molecules. We can utilize methods in the simulations of the chain molecules.

We started the simulation with pure GaN or InN without deformation of the lattice. A state free from the deformation due to incorporation of other species is a minic to a high-temperature state in which there is no trapped state by a potential energy val-

ley. The state point locates at a point on the free energy surface and then moves toward a local minimum in a course of a MC simulation. At a species-identity change the state point jumps to another place. If that place is of high energy, then acceptance ratio becomes low and accordingly the state tends to be trapped by a metastable one. Implementation of such jump moves using another high-temperature MC run devised by Frants et al. [53] is referred to as J-Walking. J-Walking method has been improved in a way that a jumped point is moved to its nearest local minimum in the energy surface by Zhou and Burne [54] and named S(Smart)-Walking. Kelires's [55] SGC simulation for Si-related alloy already included this idea approximately. With the identity change the each nearest atom is moved along the each vector connecting it and the atom for which the identity change is attempted.

Let us view the problem globally. Most tempting is muiti-canonical [56,57] type extended or generalized ensemble simulations. If we can sample without trapping by free energy local minima, of course, the phase boundary is accurately determined. In addition, if we can scan the whole free energy surface and fund out the most of local minima, then we can interpret experimental results in which the system is trapped by a local minimum other than that corresponds to the binordal line.

Let us return to the issue of the multi-valley free energy. We pointed that this phenomenon was related to the superlattice structure. Averaging over different lattice structures may correspond to sampling average from various parts of the system. Some speculated superlattice structure can be confirmed by simulation for large systems. If an effective layer-wise Hamiltonian is founded, we can perform a different scale simulation.

ACKNOWLEDEGMENTS

One of the authors (AM) thanks Dr. I. L. Maksimov for discussion during NPT'2002 workshop, which made him aware of the necessity of discussion about the symmetric nature of the intermolecure interaction (Sec. 1). This work was started during the stay of AM at University of Kansas according to a dispatch program of the Satellite Venture Business Laboratory (S-VBL) of The University of Tokushima. Some parts of this work was supported by "Research in the Future" Program from the Japan Society for the Promotion of Science in the Area of Atomic Scale Surface and Interface Dynamics and partially by S-VBL.

REFERENCES

[1] W. G. Hoover and F. H. Ree // *J. Chem. Phys.* **47** (1967) 4973.
[2] W. G. Hoover and F. H. Ree // *J. Chem. Phys.* **49** (1968) 3609.
[3] J.-P. Hansen and L. Verlet // *Phys. Rev.* **184** (1969) 151.
[4] D. Frenkel and A. J. C. Ladd // *J. Chem. Phys.* **81** (1984) 3188.
[5] A. Z. Panagiotopouls // *Mol. Phys.* **61** (1987) 813.
[6] D. Frenkel and B. Smit, *Understanding Molecular Simulation* (Academic, San Diego, 1996).
[7] D. A. Kofke and E. D. Glandt // *Mol. Phys.* **64** (1988) 1105.
[8] D. A. Kofke // *Adv. Chem. Phys.* **105** (1999) 405.
[9] R. B. Griffiths and J. C. Wheeler // *Phys. Rev. A* **2** (1970) 1047.
[10] J. G. Briano and E. D. Glandt // *J. Chem. Phys.* **80** (1984) 3336.
[11] D. A. Kofke and E. D. Glandt // *J. Chem. Phys.* **87** (1987) 4881.
[12] D. A. Kofke and E. D. Glandt // *J. Chem. Phys.* **90** (1989) 439.
[13] D. A. Kofke and E. D. Glandt // *J. Chem. Phys.* **92** (1990) 658.
[14] Y. Fan, J. E. Finn and P. A. Monson // *J. Chem. Phys.* **99** (1993) 6238.
[15] E. de Miguel, E. M. del Río and M. M. Telo da Gama // *J. Chem. Phys.* **103** (1995) 6188.
[16] C. Y. Shew and A. Yethiraj // *J. Chem. Phys.* **104** (1995) 67665.
[17] E. Lomba, M. Alvarez, L. L. Lee and N. G. Almarza // *J. Chem. Phys.* **104** (1996) 4180.
[18] L. D. Gelv and K. E. Gubbins // *Phy. Rev. E* **56** (1997) 3185.
[19] C. Caccamo, D. Costa and G. Pellicane // *J. Chem. Phys.* **109** (1998) 4498.
[20] F. A. Escobedo // *J. Chem. Phys.* **115** (2001) 5653.
[21] D. A. Kofke // *Mol. Simul.* **7** (1991) 285.
[22] M. Mehta and D. A. Kofke // *Chem. Eng. Sci.* **49** (1994) 2633.
[23] E. de Miguel and M. M. Telo da Gama // *J. Chem. Phys.* **107** (1997) 6366.
[24] M. A. Bates and D. Frenkel // *J. Chem. Phys.* **109** (1998) 6193.
[25] M. R. Stapleton and D. J. Tildesly // *J. Chem. Phys.* **92** (1990) 4456.
[26] M. A. Bates and D. Frenkel // *J. Chem. Phys.* **110** (1999) 6553.

[27] S. M. Foils // *Phys. Rev. B* **32** (1985) 14182.
[28] P. C. Kelires and J. Terfoss // *Phys. Rev. B* **63** (1989) 1164.
[29] M. Laradji, D. P. Landau and B. Dünweg // *Phys. Rev. B* **51** (1995) 4894.
[30] B. Dünweg and D. P. Landau // *Phys. Rev. B* **48** (1993) 14182.
[31] D. A. Kofke // *J. Chem. Phys.* **98** (1993) 4149
[32] D. A. Kofke // *Mol. Phys.* **78** (1993) 1331.
[33] E. J. Meijer and F. El Azhar // *J. Chem. Phys.* **106** (1997) 4678.
[34] M. de Koning, A. Anotonelli and S. Yip // *J. Chem. Phys.* **115** (2001) 11025.
[35] J. B. Sturgeon and B. B. Laird // *Phys. Rev. B* **62** (2000) 14720.
[36] P. Agrawal and D. A. Kofke // *Phys. Rev. Lett.* **74** (1995) 122, *Mol. Phys*. **85** (1995) 23.
[37] P. Agrawal and D. A. Kofke // *Mol. Phys.* **85** (1995) 43.
[38] P. J. Camp, C. P. Manson, M. P. Allen, A. A. Khare and D. A. Kofke // *J. Chem. Phys.* **105** (1996) 2837.
[39] P. Bolhuis and D. Frenkel // *J. Chem. Phys.* **106** (1997) 666.
[40] M. R. Hitchcock and C. K. Hall // *J. Chem. Phys.* **110** (1999) 11433.
[41] E. A. Escobedo and J. J. de Pablo // J. Chem. Phys. **106** (1997) 2911.
[42] E. A. Escobedo // *J. Chem. Phys.* **108** (1998) 2911.
[43] E. A. Escobedo // *J. Chem. Phys.* **110** (1999) 11999.
[44] T. Ito // *Jpn. J. Appl. Phys.* **37** (1998) L547.
[45] T. Ito, K. E. Kho and S. Das Sarma // *Phys. Rev. B* **41** (1990) 401.
[46] Y. Kangawa, T. Ito, A. Mori and A. Koukitu // *J. Cryst. Growth* **220** (2000) 401.
[47] M. K. Behbehanai, E. L. Piner, S. X. Liu, N. A. El-Masry and S. M. Bedair // *Appl. Phys. Lett.* **75** (1999) 2202.
[48] D. Doppalapudi, S. Baus, K. F. Ludwig, Jr. and T. D. Moustakas // *J. Appl. Phys.* **84** (1998) 1389.
[49] H. K. Cho, J. Y. Lee, K. S. Kim and G. M. Yang // *Appl. Phys. Lett.* **77** (2000) 247.
[50] A. M. Ferrenberg and R. H. Swenden // *Phys. Rev. Lett.* **61** (1988) 2635.
[51] A. M. Ferrenberg and R. H. Swenden // *Phys. Rev. Lett.* **63** (1989) 1195.
[52] L. K. Teles, J. Furthmüller, L. M. R. Scolfaro, J. R. Leite and F. Bechsctedt // *Phys. Rev. B* **62** (2000) 2475.
[53] D. D. Frants, D. L. Freeman and J. D. Doll // *J. Chem. Phys.* **93** (1990) 2769.
[54] R. Zhou and B. J. Berne // *J. Chem. Phys.* **107** (1997) 9185.
[55] P. C. Kelires // *Phys. Rev. Lett.* **75** (1995) 1114; *Int. J. Mod. Phys. C* **60** (1998) 11494.
[56] B. A. Berg and T. Neuhaus // *Phys. Lett. B* **267** (1991) 249.
[57] B. A. Berg and T. Neuhaus // *Phys. Rev. Lett.* **68** (1992) 9.